

ECORD Research Grant:
High-pressure melting relations of Juan de Fuca sediments and their effects on the Northern Cascade volcanic chemistry

Marina Martindale

Ph.D. student

Pacific Centre for Isotopic and Geochemical Research, Department of Earth, Ocean and Atmospheric Sciences, University of British Columbia



Aims of the Study and Cascadia Background

The northern segment of the Cascade Arc, the Garibaldi Volcanic Belt (GVB), hosts some of the youngest and hottest subducting crust globally (Syracuse et al., (2010)), along with the termination of the subducting slab at the Nootka Fault. The unique tectonic and thermal setting of the GVB may give rise to unusual melt production and lava compositions.

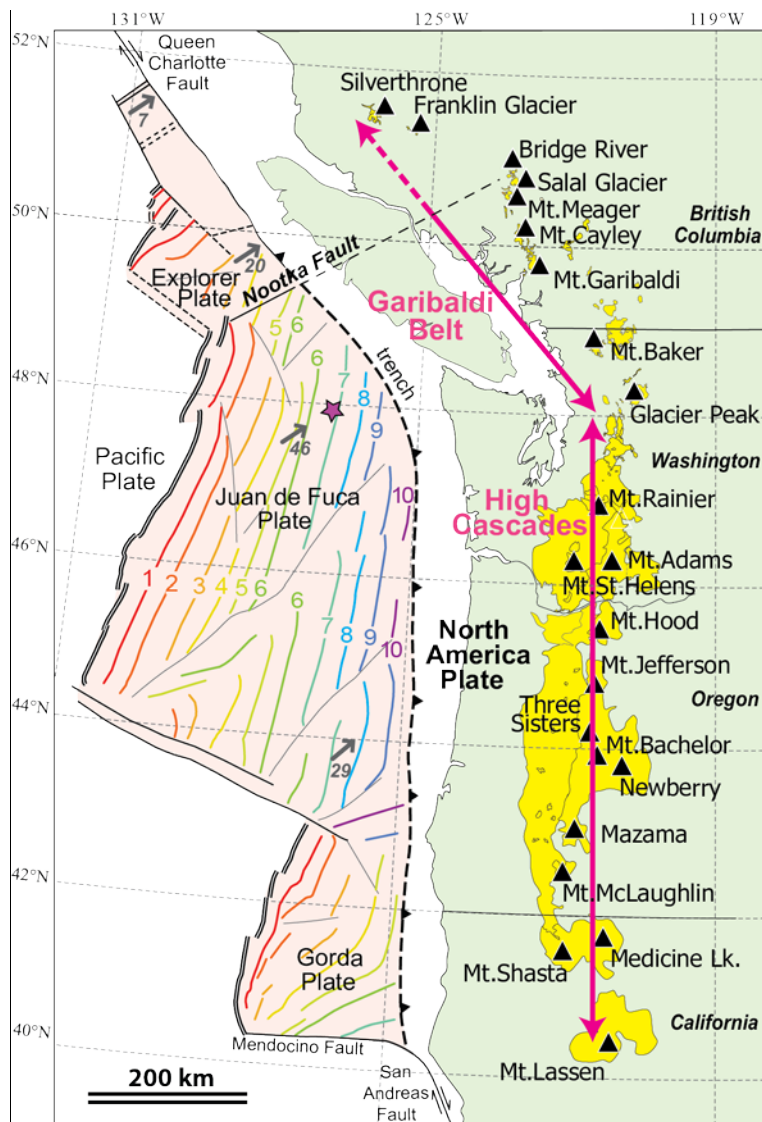


Figure 1: Map of the Cascade Arc, modified from Mullen and Weis, (2013). Major volcanic centres are shown as black triangles. Cascade Arc lavas are shown in yellow. The High Cascades and Garibaldi Volcanic Belt segments are indicated by two pink arrows.

The purple star indicates the position of the ODP drilling site (ODP-168-1027) where sediment and basaltic material originated for analyses in this project (Westbrook et al., 1994; Davis et al., 1997). Coloured lines and numbers on the subducting plate are isochrons (Wilson, 2002). Grey arrows indicate subduction direction and rate (mm/yr) obtained from McCrory et al. (2004), Riddihough and Hyndman (1991), and Braunmiller and Nabelek (2002) for a reference frame fixed relative to North America.

This project is part of a larger PhD project to determine the relative contributions of slab-input and crustal processing involved in generating evolved lavas from the Garibaldi Volcanic Belt.

The GVB is located from Glacier Peak in Washington, USA towards Mt. Meager and Silverthorne in BC, Canada (see figure 1). Mafic lavas produced in the GVB show an increase in alkalinity northwards (Green and Harry, 1999; Green and Sinha, 2005; Green, 2006; Mullen and Weis, 2013), which is not mirrored by intermediate and felsic samples (Martindale et al., 2013b; 2014). To determine the relative importance of parental magma composition and upper crustal interaction in controlling evolved lava compositions, the main subduction inputs need to be characterised. In a subduction zone, the subducting sediment exerts a large control on the generation of melt at depth (e.g., Plank and Langmuir, 1993; 1998; Elliott, 2003). Water content of the down-going slab controls when melting occurs; this water may be free water or bound in hydrous minerals of the sediment (e.g., Tatsumi et al., 1986; Poli and Schmidt, 1995; Prouteau et al., 2001; Prouteau and Scaillet, 2012). The

composition and thickness of the sediment cover also influence the temperature of the down-going slab, and the composition of the resulting melt (e.g., Gill, 1981; Hawkesworth et al., 1991; Plank and Langmuir, 1993; Elliott, 2003). The nature of this initial melt is still somewhat debated; is it a hydrous dehydration fluid, sediment melt or supercritical fluid? Both the residual phases which form during melt production, and the nature of the transport medium will determine which elements are moved from the slab to the overlying mantle wedge (e.g., Pearce, 1982; McCulloch and Gamble, 1991; Tatsumi et al., 1991; Elliott, 2003; Hermann et al., 2006; Kessel et al., 2005; Klimm et al., 2008;). A combination of subduction input composition, subduction conditions (pressure, temperature, water, fO_2) and crustal interaction ultimately produces the 'subduction signature' characteristic of subduction zones (LILE enriched compared to MORB, HFSE and HREE depleted compared to MORB; e.g., Gill, 1981; Hawkesworth et al., 1991).

Sediment subducting in the Cascadia basin is relatively juvenile compared to the Antilles, Sunda, and Java arcs which subduct sediments with a significant amount of cratonic material (Prytulak et al., 2006; Carpentier et al., 2013; 2014). However, the geochemical composition of subducting sediments does vary along the 1250 km-long Cascade Arc, highlighting the need for careful selection of appropriate sediment compositions when modelling subduction input along the arc. The southern end of the arc has been supplied with sediments that formed the Astoria Fan. The sediments are mainly terrigenous sands and clays and contain weathered material from both an old Proterozoic crust and the younger Columbia River Basalts (Prytulak et al., 2006). In contrast to the Astoria Fan sediments, the sediments deposited further north on the Juan de Fuca plate in the Cascadia basin are derived from juvenile (Carpentier et al., 2013; 2014) crust of the Coast Plutonic Complex (Mesozoic and Cenozoic in age) .

Melting sediments from the Juan de Fuca basin (figures 1, 2), under conditions specific to the GVB, will enable partition coefficients for trace elements to be determined, to assist in the modelling of primary magma generation at the northern Cascade Arc. As the GVB hosts young, hot oceanic lithosphere, the possibility of slab melts (Zellmer, 2009; Thorkelson et al., 2011; Fillmore and Coulson, 2013) contributing to the generation of melts also requires investigation. Five experiments were conducted on basalt from the subducting Juan de Fuca plate.

Methodology and Experimental Conditions

Samples

For this project, two sets of experiments were carried out. The main focus of the investigation was the melting behaviour of sediments at the northern Cascade Arc, while a smaller aspect of the investigation was the melting behaviour of the oceanic basalt during subduction.

Sample powders are derived from drill-cores from Ocean Drilling Program site ODP-168-1027 (see figure 1). The site is located ~200km from the Vancouver Island coast and drilled through a 606m thick sedimentary pile and 26m of 3.56Ma basement so spans a 3.5Ma time period (Davis et al., 1997). The sediment sample (ODP 168-1027-B-23X-1-42) is a split from the geochemical analyses of the Cascadia basin by Carpentier et al., (2013, 2014), and composes ~60% sand, 40% silt quartz-plagioclase with minor biotite, amphibole and rock fragments with trace amounts of calcite and LOI: 6.27 wt.% (H_2O to be determined). The sample was chosen as it closely matches the calculated bulk-average sediment pile from ODP

drill site 146-1027, minus a volumetrically minor basal carbonate layer (calculated using chemical data from Carpentier et al., 2013). The carbonate layer was discounted due to the effect on sediment melting behaviour carbonates impose; see Skora et al., (submitted) for discussion. The 3.56Ma basalt sample (ODP 168-1027-C-4R-3) is a microcrystalline sparsely phyrific olivine-plagioclase basalt with trace amounts of alteration minerals such as pyrite, aragonite, celadonite etc. with H₂O of 2.9% (Davis et al., 1997). A basalt sample from the upper portion of the oceanic slab was chosen due to its relatively high K₂O content (0.22 wt.%), allowing for efficient melting; it is believed the upper portion of the slab is extensively weathered by seawater interaction, thus is a major source of dehydration fluids during subduction (Staudigel et al., 1995; Elliott, 2003).

Both sediment and basalt samples were crushed in an agate pestle and mortar, and had no 'extra' water added (but still contained structurally-bound water/volatiles of the natural sample), also no 'doping' of the powders to increase trace element abundances was performed before the powders were used as the melting protolith; see Martindale et al., (2013a) and Carter et al., (submitted) for discussions on the effect of water and doping in experimental procedures.

Experimental set-up

Experiments were conducted at the Experimental Petrology Laboratory at the Department of Earth Sciences, University of Bristol (UK) over the course of six weeks, from April to June 2014. Funds from ECORD were used to cover the cost of the experimental materials, and use of equipment at the University of Bristol, which is not available at the Department of Earth, Ocean and Atmospheric Sciences, University of British Columbia. Experimental design and set-up were supervised by Dr. Richard Brooker and Professor Jon Blundy at the University of Bristol.

Sample powders were loaded into single 3mm wide capsules which were acid-cleaned and annealed before loading. For <1000°C runs, Au capsules were used to minimise alloying with Fe, which can occur with Au-Pd capsules; however, as Au₇₀-Pd₃₀ capsules have a higher melting point than Au capsules, Au₇₀-Pd₃₀ was used for the single 1100°C run. The loaded capsules were measured before and after welding with a PUK microwelder (which ensures the sample remains below boiling temperature at all times due to its highly localised heat source) to monitor any possible water loss from the sample.

Pressure and temperature conditions for the experiments were guided by the Syracuse et al., (2010) *D80* model of slab thermal structure (see table 1; figure 2) with durations of 1–10 days depending on temperature (guided by Klimm et al., (2008); balance between higher H⁺ loss and greater equilibrium at longer run times). Experiments were conducted in a half-inch, end-loaded piston cylinder apparatus, with an assembly of salt–Pyrex outer sleeves, crushable magnesium-oxide spacers and a graphite furnace. A friction–correction of 3% was applied to the experimental pressure (McDade et al., 2002). Temperatures were measured by calibrated W₉₅Re₅–W₇₅Re₂₅ (Type D) thermocouples inserted axially into the assembly. Sample capsules measured no more than 6mm and were placed at the calculated hotspot of the experimental setup, reducing the thermal gradient within the capsule, allowing for a more accurate measurement of temperature. All experiments were unbuffered for *f*O₂, largely due to the redox state of subduction zones being relatively unknown, but estimated around QFM±2 (Prouteau and Scaillett., 2013). Oxygen fugacities also vary between apparatus and capsule material due to differences in hydrogen permeability; see Truckenbrodt et al., (1997); Jakobsson (2012); Prouteau and Scaillett (2013) for discussions. In-house estimates of the

fO_2 of the piston cylinder apparatus used is $NNO+2(\pm 1)$ for similar pressure-temperature conditions as those used in this study. Isobaric quenching was achieved by turning off the power and maintaining run pressure until temperature had dropped below $25^\circ C$. The run-product capsules were mounted in epoxy resin and polished with abrasive paper to expose the contents of the capsule, and polished for subsequent microbeam and LA-ICPMS analysis.

Run conditions

Experimental runs were conducted to explore melting behaviour of the subducting Juan de Fuca slab in the northern Cascade Arc, according to thermal models by Syracuse et al., (2010); see Table 1 and figure 2.

Table 1: Experimental run-product pressure-temperature conditions								
P (GPa)	T (°C)	Sediment	Basalt		P (GPa)	T (°C)	Sediment	Basalt
2.5	750	◆			3	800	◆	■
2.5	800	◆	■		3	850	◆	
2.5	850	◆			3	900	◆	■
2.5	900	◆			3	950	◆	■
2.5	950	◆			3	1000	◆	■
2.5	1000	◆			3	1100	◆	
Symbols (as in figure 2) indicate an experimental run was performed for that starting material under the indicated P-T conditions					3.5	1000	◆	

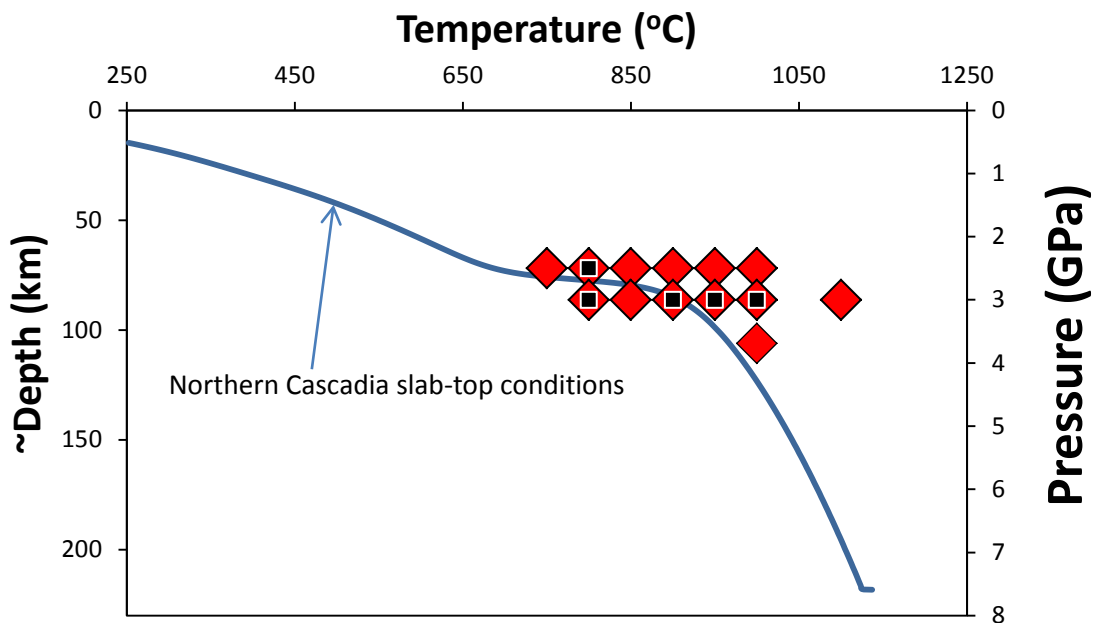


Figure 2: Pressure-temperature conditions of the surface of the subducting Juan de Fuca plate in the Cascadia subduction zone. Blue line is model D80, northern Cascadia; Syracuse et al., (2010). Red diamonds indicate sediment-protolith (ODP 168-1027-B-23X-1-42) experimental runs. Black squares indicate basaltic-protolith (ODP 168-1027-C-4R-3) experimental runs.

Initial Results

Phase relations of natural sediments from the Juan de Fuca basin were investigated experimentally at 2.5GPa-3.5GPa and 750-1100°C and Juan de Fuca basalt was investigated at 2.5-3GPa and 800-1000°C.

At 3GPa, sediment melting begins ~800°C whereas melting begins ~750°C at 2.5GPa. The proportion of garnet is fairly consistent at ~30% in all runs from 2.5-3.5GPa and 750-1100°C. The lower pressure experimental runs at 2.5GPa experience a higher melt percentage for a given temperature than 3GPa and 3.5GPa runs. The SiO₂ phase generally decreases with increasing temperature in all runs, as does amphibole and pyroxene (see figure 3). Minor amounts of an Al₂SiO₅ phase and Fe-Ti-oxides are present in all runs.

Sediment (ODP 168-1027-B-23X-1-42) Melt Products

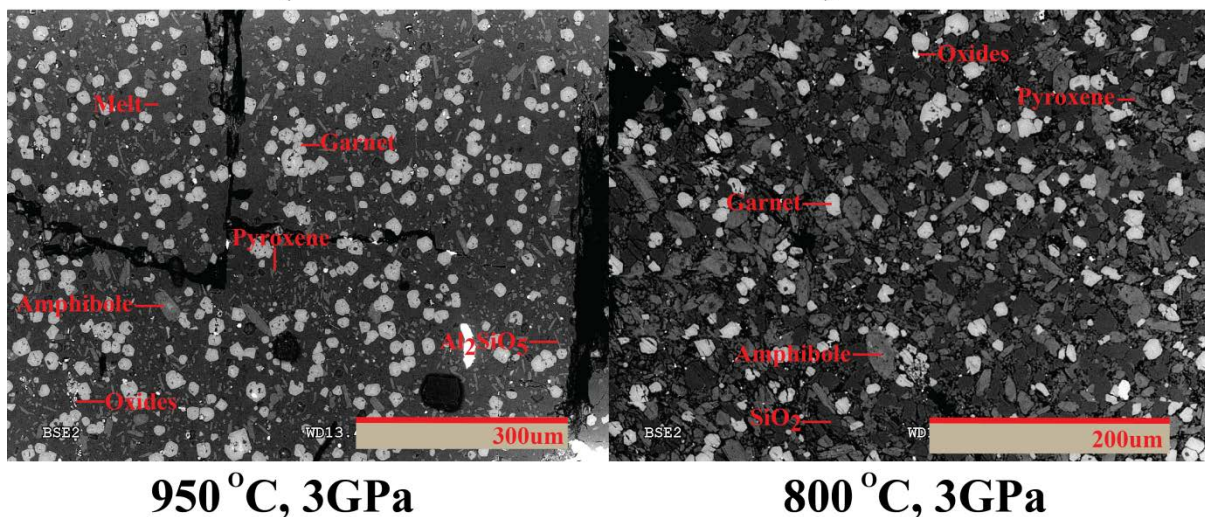
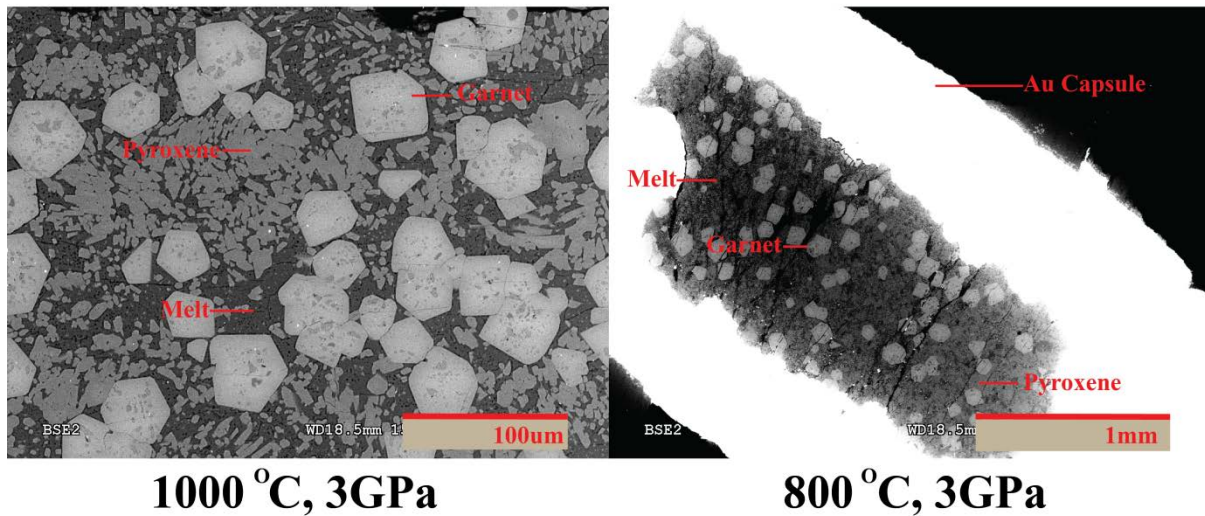


Figure 3: SEM images of sediment-melt run products. Left) 950°c, 3GPa: melt, garnet, pyroxene, Al₂SiO₅. Right) 800°c, 3GPa: garnet, pyroxene Al₂SiO₅, SiO₂, melt.

The Juan de Fuca basalt produced an eclogitic assemblage of Na-rich pyroxene, garnet and vesicular melt in all experimental runs, with melting commencing between 800-900°C. At 3GPa the proportion of garnet was fairly consistent at ~45%, with pyroxene decreasing from ~50% to 20% and melt percentage increasing with increasing temperature to a maximum of ~30% at 1000°C (see figure 4). An Al₂SiO₅ phase was present below 950°C, and minor rutile was found in all runs. Garnets produced were generally larger (<100 microns) than those produced from the sediment starting material (<30 microns) possibly due to kinetic effects or from seeding from old crystal cores which may have been present in the basaltic starting material.

Basalt (ODP 168-1027-C-4R-3) Melt Products



1000 °C, 3GPa

800 °C, 3GPa

Figure 4: SEM images of basalt-melt run products. Left) Basalt melt 1000°C 3GPa; Right) Basalt melt 800°C 3GPa; both produce an eclogite assemblage of pyroxene, garnet and melt.

Further Work

Detailed analyses of the phases which formed in each experimental run will be carried out to determine melting reactions of both the sediment and basalt of the Juan de Fuca plate under Cascadia-like conditions. Microprobe and LA-ICP-MS analyses of major and trace elements of both the melt and minerals are now underway at the University of British Columbia for mass-balance calculations and determination of melt-solid partition coefficients. The behaviour of the trace elements during melting, by analyses of the glass, will help determine the nature of the chemical transport mechanism at specific subduction conditions. The data produced from this study will aid modelling subduction input to the northern Cascade Arc and help explain primary melt production in Cascadia and other 'hot' subduction zones globally. The results of this study will be presented at an international conference and published as a paper in 2015.

Budget

The scope of the original project expanded to include a greater number of experiments to further help constrain melting behaviour under a greater range of pressures and temperatures as well as conducting experiments on Juan de Fuca basalt. In turn, extra time was needed to conduct all the experiments resulting in higher costs than originally planned.

Original budget:

12 x £100 melting experiments: £1200

Two weeks accommodation in Bristol at £500

Final budget:

25 x £100 melting experiments at the University of Bristol: £2500

Six weeks accommodation in Bristol: £711

Total cost: £3211 (~4059€)

Total requested from ECORD: 1900€**

***Flights (Vancouver-Bristol) and local transport were covered by external funding (Professor D. Weis, Ph.D. Advisor NSERC Discovery Grant). Microprobe and laser-ablation ICP-MS analyses can be carried out in-house at the Pacific Centre for Isotopic and Geochemical Research (PCIGR) at University of British Columbia and is covered by the same sources of funding.*

I'd like to take the chance to thank ECORD for the financial support, which made this project possible. The opportunity to conduct these experiments, using the renowned facilities at the University of Bristol Experimental Petrology Laboratory, with guidance from experts in experimental petrology has really added another dimension to my Ph.D. thesis that would otherwise not be available.

References

- Braunmiller, J., Nabelek, J. (2002) Seismotectonics of the Explorer region. *Journal of Geophysical Research*, 107(B10), 2208, doi:10.1029/2001JB000220.
- Bureau, H., Keppler, H. (1999) Complete miscibility between silicate melts and hydrous fluids in the upper mantle: experimental evidence and geochemical implications. *Earth and Planetary Science Letters*, 165(2), 187-196.
- Carpentier, M., Weis, D., Chauvel, C. (2013) Large U loss during weathering of upper continental crust: The sedimentary record. *Chemical Geology*, 340, 91–104.
- Carpentier, M., Weis, D., Chauvel, C. (2014) Fractionation of Sr and Hf isotopes by mineral sorting in Cascadia Basin terrigenous sediments. *Chemical Geology*, 382, 67–82.
- Carter, L., Skora, S., Blundy, J., de Hoog, J.C.M., Elliott, T. (2014) An experimental study of trace element fluxes from subducted oceanic crust. *Journal of Petrology*, in revision.
- Davis, E. E., Fisher, A. T., Firth, J. V., Fox, P. J., Allan, J. (1997) Hydrothermal circulation in the oceanic crust: Eastern flank of the Juan de Fuca Ridge. *Proceedings of ODP, Initial Reports*, 168, pp. 1-470.
- Elliott, T. (2003) Tracers of the slab. In: *Inside the subduction factory*. Eiler, J. (ed.), American Geophysical Union Geophysical Monograph, 138, 23–45
- Fillmore, J., Coulson, I. M. (2013) Petrological and geochemical constraints on the origin of adakites in the Garibaldi Volcanic Complex, southwestern British Columbia, Canada. *Bulletin of Volcanology*, 75(7), 1-23.
- Gill, J. G. (1981) *Orogenic Andesites and Plate Tectonics*. Springer Verlag, Berlin.
- Green, N. L., Harry, D. L. (1999) On the relationship between subducted slab age and arc basalt petrogenesis, Cascadia subduction system, North America. *Earth Planet Science Letters*, 171, 367–381.
- Green, N. L., Sinha, A. K. (2005) Consequences of varied slab age and thermal structure on enrichment processes in the sub-arc mantle of the northern Cascadia subduction system. *Journal of Volcanology and Geothermal Research*, 140, 107-132.
- Green, N. L. (2006) Influence of slab thermal structure on basalt source regions and melting conditions: REE and HFSE constraints from the Garibaldi volcanic belt, northern Cascadia subduction system. *Lithos*, 87, 23–49.
- Hawkesworth, C. J., Hergt, J. M., Ellam, R. M., Mc Dermott, F. (1991) Element fluxes associated with subduction related magmatism. *Philosophical Transactions of the Royal Society of London. Series A: Physical and Engineering Sciences*, 335(1638), 393-405.
- Hawkesworth, C.J., Gallagher, K., Hergt, J.M., McDermott, F. (1993) Mantle and slab contributions in arc magmas. *Annual Review of Earth and Planetary Science*, 21, 175–204.
- Hermann, J., Spandler, C., Hack, A., Korsakov, A. V. (2006) Aqueous fluids and hydrous melts in high-pressure and ultra-high pressure rocks: implications for element transfer in subduction zones. *Lithos*, 92(3), 399-417.
- Hermann, J., Spandler, C. J. (2008) Sediment melts at sub-arc depths: an experimental study. *Journal of Petrology*, 49, 717–740.
- Hermann, J., Rubatto, D. (2009) Accessory phase control on the trace element signature of sediment melts in subduction zones. *Chemical Geology*, 265, 512–526.
- Jakobsson, S. (2012) Oxygen fugacity control in piston-cylinder experiments. *Contributions to Mineralogy and Petrology*, 164(3), 397-406.
- Kessel, R., Schmidt, M.W., Ulmer, P., Pettker, T. (2005) Trace element signature of subduction-zone fluids, melts and supercritical liquids at 120–180 km depth. *Nature*, 437, 724–727.
- Klimm, K., Blundy, J. D., Green, T. H. (2008) Trace element partitioning and accessory phase saturation during H₂O-saturated melting of basalt with implications for subduction zone chemical fluxes. *Journal of Petrology*, 49, 523–553.
- Martindale, M., Skora, S., Pickles, J., Elliott, T., Blundy, J., Avanzinelli, R. (2013) High pressure phase relations of subducted volcanoclastic sediments from the west Pacific and their implications for the geochemistry of Mariana arc magmas. *Chemical Geology*, 342, 94-109.
- Martindale, M., Mullen, E., Weis, D. (2013) Geochemistry of Garibaldi Lake andesites and dacites indicates crustal contamination involved in formation of Northern Cascade arc lavas. *AGU Fall Meeting Abstracts*, 2751.
- Martindale, M., Mullen, E., Weis, D. (2014) Geochemical Constraints on the Origin of Evolved Magmas in the Northern Cascades. *Goldschmidt Abstracts*, 1604.

- McCrory, P. A., Blair, J. L., Oppenheimer, D. H. Walter, S. R. (2004) Depth to the Juan de Fuca slab beneath the Cascadia subduction margin: A 3-D model for sorting earthquakes [CD-ROM]. U.S. Geological Survey Data Series, DS-91.
- McDade, P., Wood, B.J., van Westrenen, W., Brooker, R., Gudmundsson, G., Soular, H., Najorka, J., Blundy, J. (2002) Pressure corrections for a selection of piston-cylinder cell assemblies. *Mining Magazine*, 66, 1021–1028.
- Mullen, E. K., Weis, D. (2013) Sr-Nd-Hf-Pb isotope and trace element evidence for the origin of alkalic basalts in the Garibaldi Belt, northern Cascade arc. *Geochemistry, Geophysics, Geosystems*, 14(8), 3126-3155.
- Pawley, A. R., Holloway, J. R. (1993) Water sources for subduction zone volcanism: New experimental constraints. *Science*, 260(5108), 664-667.
- Pearce, J.A. (1982) Trace element characteristics of lavas from destructive plate boundaries. In: Thorpe, R.S. (Ed.), *Andesites*. John Wiley, New York, pp. 525–548.
- Pearce, J. A., Peate, D. W. (1995) Tectonic implications of the composition of volcanic arc magmas. *Annual Review of Earth Planetary Science*, 23, 251–285.
- Plank, T., Langmuir, C. H. (1993) Tracing trace-elements from sediment input to volcanic output at subduction zones. *Nature*, 362, 739–743.
- Plank, T., Langmuir, C. H. (1998) The chemical composition of subducting sediment and its consequences for the crust and mantle. *Chemical Geology*, 145(3), 325-394.
- Poli, S., Schmidt, M. W. (1995) H₂O transport and release in subduction zones: experimental constraints on basaltic and andesitic systems. *Journal of Geophysical Research: Solid Earth*, (1978–2012), 100(B11), 22299-22314.
- Prouteau, G., Scaillet, B., Pichavant, M., Maury, R. (2001) Evidence for mantle metasomatism by hydrous silicic melts derived from subducted oceanic crust. *Nature*, 410(6825), 197-200.
- Prouteau, G., Scaillet, B. (2012) Experimental Constraints on Sulphur Behaviour in Subduction Zones: Implications for TTG and Adakite Production and the Global Sulphur Cycle since the Archean. *Journal of Petrology*, 54, 183–213.
- Prytulak, J., Vervoort, J. D., Plank, T., Yu, C. (2006) Astoria Fan sediments, DSDP site 174, Cascadia Basin: Hf–Nd–Pb constraints on provenance and outburst flooding. *Chemical Geology*, 233(3), 276-292.
- Riddihough, R. P., Hyndman, R. D. (1991) The modern plate tectonic regime of the continental margin of western Canada, in *Geology of the Cordilleran Orogen in Canada*, 2, pp. 435-455, eds. Gabrielse, H. & Yorath, C.J., Geological Survey Canada, Geology of Canada.
- Skora, S., Blundy, J. (2010) High-pressure hydrous phase relations of radiolarian clay and implications for the involvement of subducted sediment in arc magmatism. *Journal of Petrology*, 51, 2211–2243.
- Skora, S. Blundy, J., Brooker, R., de Hoog, J.C.M. (2014) Hydrous phase relations and trace element partitioning behaviour in calcareous sediments at subduction zone conditions. *Journal of Petrology*, in revision.
- Staudigel, H., Davies, G. R., Hart, S. R., Marchant, K. M., Smith, B. M. (1995) Large scale isotopic Sr, Nd and O isotopic anatomy of altered oceanic crust: DSDP/ODP sites 417/418. *Earth and Planetary Science Letters*, 130(1), 169-185.
- Syracuse, E. M., van Keken, P. E., Abers, G. A. (2010) The global range of subduction zone thermal models. *Physics of the Earth and Planetary Interiors*, 183, 73-90.
- Tatsumi, Y., Hamilton, D. L., Nesbitt, R. W. (1986) Chemical characteristics of fluid phase released from a subducted lithosphere and origin of arc magmas: evidence from high-pressure experiments and natural rocks. *Journal of Volcanology and Geothermal Research*, 29(1), 293-309.
- Tatsumi, Y., Murasaki, M., Arsadi, E. M., Nonda, S. (1991) Geochemistry of Quaternary lavas from NE Sulawesi: transfer of subduction components into the mantle wedge. *Contributions to Mineralogy and Petrology*, 107(2), 137-149.
- Tatsumi, Y., Kogiso, T. (1997) Trace element transport during dehydration processes in the subducted oceanic crust: 2. Origin of chemical and physical characteristics in arc magmatism. *Earth and Planetary Science Letters*, 148(1), 207-221.
- Thorkelson, D., Madsen, J., Sluggett, C. L. (2011) Mantle flow through the Northern Cordilleran slab window revealed by volcanic geochemistry. *Geology*, 39, 267–270.
- Truckenbrodt, J., Ziegenbein, D., Johannes, W. (1997) Redox conditions in piston cylinder apparatus: The different behavior of boron nitride and unfired pyrophyllite assemblies. *American Mineralogist*, 82, 337-344.
- Westbrook, G. K., Carson, B., Musgrave, R.J. (1994) *Proceedings of ODP, Initial Reports*, 146 (Pt.1). Ocean Drilling Program, College Station, TX.
- Wilson, D. S. (2002) The Juan de Fuca plate and slab: Isochron structure and Cenozoic plate motions. The Cascadia subduction zone and related subduction systems. pp. 9-12 US Geological Survey, open-file report 02-328 and Geological Survey Canada, open file 4350.
- van Keken, P. E., Kiefer, B., Peacock, S. M. (2002) High-resolution models of subduction zones: Implications for mineral dehydration reactions and the transport of water into the deep mantle. *Geochemistry, Geophysics, Geosystems*, 3(10).
- Zellmer, G. F. (2009) Petrogenesis of Sr-rich adakitic rocks at volcanic arcs: insights from global variations of eruptive style with plate convergence rates and surface heat flux. *Journal of the Geological Society*, 166(4), 725-734.